# Analytical Modeling of 9-150 kHz EMI in Single-Phase PFC Converter

Esfetanaj, Naser Nourani; Peyghami, Saeed; Wang, Huai; Davari, Pooya

*Published in:*
Proceedings of IECON 2019 - 45th Annual Conference of the IEEE Industrial Electronics Society

*Publication date:*
2019

*Document Version*
Accepted author manuscript, peer reviewed version

# Analytical Modeling of 9-150 kHz EMI in Single-Phase PFC Converter

Naser Nourani Esfetanaj, Saeed Peyghami, Huai Wang, Pooya Davari
Department of Energy Technology, Aalborg University, Aalborg, Denmark
nne@et.aau.dk, sap@et.aau.dk, hwa@et.aau.dk, pda@et.aau.dk

***Abstract*—This paper proposes an analytical approach for modeling low frequency Differential Model (DM) Electromagnetic Interference (EMI) noise of single-phase Power Factor Correction (PFC) converters within 9-150 kHz frequency range. In order to develop analytical model of the DM EMI noise, the switching function model of the converter is calculated utilizing double Fourier analysis including its input closed-loop impedance model. Notably, the analytical modeling includes Line Impedance Stabilization Network (LISN) circuit and EMI receiver. A 1 kW single-phase boost PFC converter prototype is used for validation of the proposed EMI modeling technique.**

***Keywords—Low Frequency EMI, Analytical Modeling, Boost PFC Converter, Equivalent Circuit Model.***

## I. INTRODUCTION

In recent years, due to the global shift of energy paradigm to carbon-free technologies, the penetration of grid-tied power electronic systems has dramatically increased. Applying such technologies along with smart metering results in smarter grid operation, which brings suitable solutions in managing demand and generation sides and guarantee versatile operation of the power grid in distributed manner. The development of smart grid technologies introduces new issues directly associated with the assurance of the Electromagnetic Compatibility (EMC) of these specific systems [1]. Providing smart grid services for power systems usually requires the application of the susceptible smart metering equipment connected to power electronic converters, generating high-level EMI [2], [3]. Grid-tied power electronic converters can be generally classified into four categories of frequency including: 1) the converters which generate harmonics under 2 kHz, such as line commutated rectifiers, 2) the converters which are operating at frequencies above 20 kHz e.g., low power single-phase active rectifiers, 3) the converters which operate at frequencies more than 9 kHz, such as three-phase Pulse Width Modulated (PWM) rectifiers with low power, and 4) the converters which are operating at switching frequency less than 9 kHz such as medium and high power PWM rectifiers. According to this classification, most converters have a switching frequency between 2 and160 kHz [4]. In order to ensure the power electronic systems EMC, the generated noise emissions should be controlled within the specific limits following international standards [5]. However, as it is shown in Fig. 1, the EMI frequency ranges under 2 kHz and above 150 kHz are well covered with multitude standards, there are no general standards for the noise emission frequency range of 2-150 kHz [6]. The given gap of standardization for EMI in the frequency range from 2 kHz up to 150 kHz actually

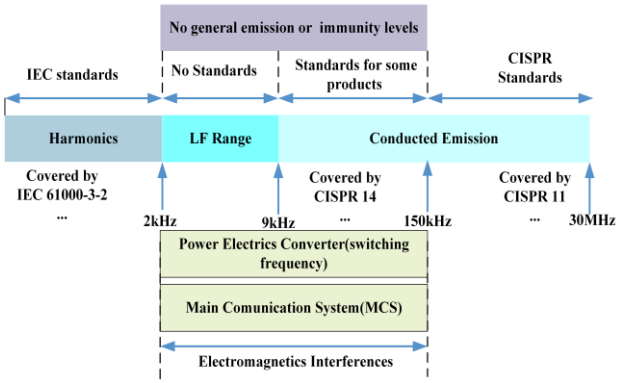


Fig. 1. Harmonic and conducted EMI frequency range classified by IEC for electrical network [6].

leads to challenging to the interferences caused by power electronic converters [7]. Extensive penetration of the power electronic converters and Main Communication System (MCS) due to their technological advancement within this range are the main reason that this frequency range is really of high importance. For instance, Photovoltaic (PV) converters [8], the electric vehicle onboard battery chargers [9], and laptop chargers [10], have an operating frequency within frequency range from 2 kHz to 150 kHz. MCS especially smart meters that measures consumption or production of electrical energy is essential in any smart grid and their importance is increasing due to the energy management requirements at both service supplier and consumer sides. Moreover, according to Fig. 1 most MCS intentionally communicate within the frequency range in which the power electronics generats non-intentional emission. Furthermore, recently there are several noise emission interferences reported for different power converters in this frequency range [11], [12]. In [11], EMI behavior of several different Battery Electric Vehicles (BEV) have been analyzed implying that the noise emission occurs within 9-150 kHz frequency ranges and more importantly, their behavior depends on the vehicle charging state.

Notably, developing suitable equivalent circuit model of a power converter is one of the important stages in analyzing frequency behavior and consequently EMI issues. Utilizing power converter models not only can speed up the design process, prevent timely trial and error, empirical measurements and reduce cost, but also it is the only feasible method to study large scale systems. This is of special importance when it comes to power distribution networks in which several power converters are connected to the grid. So far, majority of

conducted research studies are based on simulation models considering frequencies above 150 kHz [13], [14]. However, utilizing simulation tools is not computationally efficient.

Thereby, there is a need for suitable analytical modeling of EMI emission based on power converter switching function and closed loop impedance models. Employing power converter models can be beneficial and cost-effective for EMI studies in power converters especially in large scale systems such as future smart grids. Therefore, in order to investigate EMI in this frequency range, this paper proposes an analytical modeling approach for differential noise source in a single-phase boost PFC converter. In the following, the proposed analytical modeling of EMI in the boost PFC converter is presented in Section II. A comprehensive comparative analysis including analytical models, simulations, experiments are provided in Section III. Finally, the outcomes are summarized in Section IV.

## II. Analytical Modeling of Low Frequency EMI

This section provides the analytical model of a single-phase boost PFC in the following.

### A. Equivalent circuit model

EMI is one of the main challenges of grid-tied power electronic systems. Developing a suitable equivalent circuit model of the power converter is one of the important stages in analysing frequency behavior and consequently managing EMI issues. In this respect, equivalent circuit model investigation is started by modelling of high-frequency current injected by the converter to the grid. Many kinds of switches in power electronic converters are known as a source of EMI and harmonics, hence, knowing the waveform of the voltage across the switches provides many technical advantages for EMI analytical modelling of EMI. The general structure of implemented PFC rectifier with the LISN and EMI receiver is illustrated in Fig. 2. Notably, PFC is the most common utilized AC-DC conversion stage for single-phase power electronic applications. Thereby, a boost PFC converter has been chosen in this paper for the case study. The voltage across the switch in Continuous Conduction Mode (CCM) operation is shown in Fig. 3. The voltage across the switch waveform created by comparing the output of the full bridge diode rectifier voltage with the modulated switching signal of the converter. For calculating the frequency spectrum of the voltage across the switch, a double Fourier transform is employed by using (1).

$$A_{mn} + jB_{mn} = \frac{1}{2\pi^2}\int_{-\pi}^{+\pi}\int_{-\pi.M.|\mathrm{Cos}(y)|}^{\pi.M.|\mathrm{Cos}(y)|} U_{dc} e^{j(m.x+ny)} \tag{1}$$

where, $U_{dc}$ and $M$ stating the output voltage DC value and the modulation index, respectively. A general closed-form solution of the voltage across the switch can be expressed as (2), where, it comprise of a DC offset value, baseband harmonics, carrier group harmonic and sideband harmonics.

$$\begin{aligned} u_s(t) &= \frac{A_{00}}{2} + \sum_{n=1}^{\infty}[A_{0n}\cos(nw_0 t) + B_{0n}\sin(nw_0 t)] \\ &+ \sum_{m=1}^{\infty}[A_{mo}\cos(mw_c t) + B_{m0}\sin(mw_c t)] \\ &+ \sum_{m=1}^{\infty}\sum_{\substack{n=-\infty \\ n\neq 0}}^{\infty} A_{mn}\cos([mw_c + nw_c]t) + B_{mn}\sin([mw_c + nw_c]t) \end{aligned} \tag{2}$$

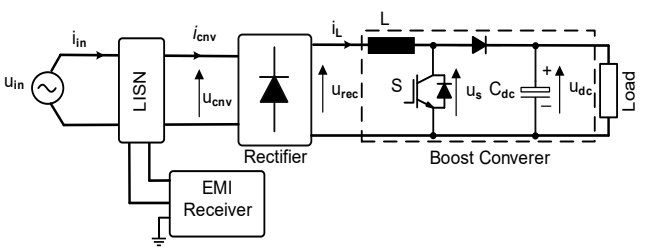


Fig. 2. Block diagram of a single-phase boost PFC converter including LISN and EMI receiver.

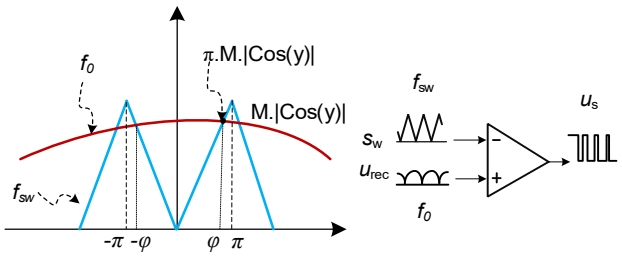


Fig. 3. The voltage across the switch ($u_s$) in CCM mode operation in a boost PFC converter.

with $m$ and $n$ representing the carrier group and baseband group indices, respectively. The fundamental and carrier angular frequencies are stated as $w_c$ and $w_0$. $A_{0n}$, $B_{0n}$, $A_{m0}$, $B_{m0}$, $A_{mn}$ and $B_{mn}$ denote the harmonic coefficients, which should be obtained according to the associated modulation methods applied to the boost PFC converter. Moreover, calculating of Fourier coefficients need to reformulate the PWM process such that it can be described by a two-dimensional function. This is shown in Fig. 3 for PWM modulation. In this respect, the Fourier coefficients are calculated according to (1). Modulation index can be calculated by (3).

$$M = \frac{U_{in}}{U_{dc}} = \frac{230\sqrt{2}}{400} \tag{3}$$

Particular values of the index variables $m$ and $n$ can be calculated by using (2). The DC offset in (2) is evaluated for $m = n = 0$ as:

$$A_{00} + jB_{00} = \frac{A_{00}}{2} = \frac{2MU_{dc}}{\pi} \tag{4}$$

Baseband and fundamental harmonics can be obtained by substituting the index variable of $m = 0$ in (2) as:

$$A_{on} + jB_{on} = \frac{MU_{dc}}{\pi}(-ni + 2e^{\frac{n\pi i}{2}} + ine^{n\pi i})\frac{-e^{-n\pi i}(1+e^{n\pi i})}{n^2-1} \tag{5}$$

Moreover, it has to be noticed that carrier harmonics can be calculated with the index variable of $n = 0$ in (2) as:

$$A_{mo} + jB_{mo} = \frac{8U_{dc}}{\pi^2}\frac{1}{m}\sum_{\substack{k=1 \\ k=odd}}^{\infty}\frac{J_k(m\pi M)}{k} \tag{6}$$

Finally, with values of the index variables, $m \neq 0$, $n \neq 0$ in (2), sideband harmonics is obtained by using (7).

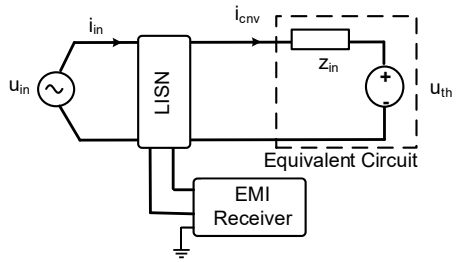


Fig. 4. Thevenin equivalent circuit of the simplified boost PFC converter.

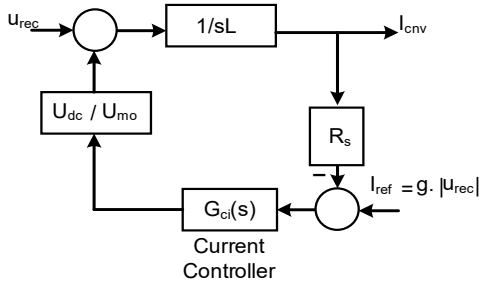


Fig. 5. High-frequency dynamics block diagram of single-phase boost PFC converter adopted from [16].

$$A_{mn} + jB_{mn} = \frac{2.U_{dc}}{\pi^2}\frac{1}{jm}\times \sum_{k=1}^{\infty} J_k(m\pi M)(j^k - j^{-k})\left(\frac{(\sin(\frac{k-n}{2})\pi)}{k-n} + \frac{(\sin(\frac{k+n}{2})\pi)}{k+n}\right) \quad (7)$$

A simplified case study structure with Thevenin equivalent circuit is shown in Fig. 4. The Thevenin equivalent voltage, $u_{th}$, is obtained from the double Fourier transform of the voltage across the switch. The voltage across the switch is the resultant of PWM modulation which is associated with the PWM modulation and output voltage of diode rectifier which is calculated by (1) as $u_s$(t). Moreover, in order to take into across the impact of full-bridge diode rectifier (see Fig. 2) on the voltage across the switch and consequently on the grid current, the Furrier transform of its switching function should be analyzed. Since, the switching function of the diode rectifier is a square ware signal, its Furrier transform can be obtained by using:

$$u_d(t) = \sum_{\substack{h=1 \\ h=odd}}^{\infty} \frac{2}{h\pi}\sin(\frac{h.\pi}{2})\cos(w_0 ht) \quad (8)$$

Thereby, the equivalent Thevenin voltage from grid side point of view in Fig. 4 is obtained by using (9).

$$u_{th}(t) = u_d(t)u_s(t) \quad (9)$$

For calculating the current harmonics injected by the boost PFC, its closed-loop input impedance is modelled. High-frequency dynamic model block diagram of the single-phase boost PFC converter is shown in Fig. 5. The input impedance of the PFC converter based on a large signal model can be obtained by using (10):

$$z_{in} = \frac{U_{cnv}}{I_{cnv}} = \frac{sL + \frac{R_s}{U_{mo}}(U_{dc}G_{ci})}{1 + \frac{1}{U_{mo}}(gU_{dc}G_{ci})} \quad (10)$$

where, $U_{dc}$ is the output dc voltage, $U_{mo}$ is the peak-to-peak value of the PWM signal, and $g$ is a constant value. More details regarding the modelling of the boost PFC converter's closed loop impedance has been discussed in [16]. Finally, the analytical EMI of boost PFC can be obtained by calculating the current harmonics using:

$$i_{cnv} = \frac{u_{th}}{z_{in}} \quad (11)$$

### *B. LISN and EMI receiver model*

To measure the conducted EMI noise voltage, the standard LISN is considered at the input terminal of the converter to create a fixed impedance, coupling power converter to the grid in high frequency, and provide a noise measurement terminal. Moreover, this provides the same condition of test for repeating EMI measurement in different conditions. Thereby, in order to model the EMI emissions, the analytical equivalent circuit model of LISN and EMI receiver should be developed as well. The current noise of converter flows into the LISN and then into the EMI receiver to measure the noise emission. It has to be noticed that analytical relation between the output current of rectifier and EMI receiver branch at LISN current should be calculated by solving the electrical circuit. This relation is presented in (12).

$$i_{rec} = \frac{A}{B}i_{cnv} \quad (12)$$

where $A$ and $B$ are defined by using (14) and (15) respectively.

$$A = L_1L_2C_1C_2s^4 + R_2C_1C_2(L_2 + L_1)s^3 + R_2C_1C_2(L_2 + L_1)s^2 \quad (13)$$

$$B = C_1C_2(R_2 + L_2L_1)s^4 + C_1(C_2L_2R_2 + L_1)s^3 + C_1R_1(L_2 + L_2C_2 + R_2C_2)s^2 + (R_1C_1 + L_2C_2 + R_2C_2)s + 2 \quad (14)$$

The EMI receiver voltage is calculated by (15).

$$u_{meas} = R_1 i_{rec} \quad (15)$$

Furthermore, the LISN/AMN circuit per line for Band A according to CISPR 16 is shown in Fig. 6 (a), where its impedance is shown in Fig. 6 (b) illustrating LISN impedance for $f$ < 150 kHz. According to CISPR 16 standard for Band A, the bandwidth of EMI receiver filter should be chosen as 200 Hz[17]. Moreover, a 4th order Butterworth filter is used for modeling of this filter, and EMI is measured by sweeping RBW filter in the frequency range of band A range. By using EMI peak measurement equation from [18], the EMI values can be calculated by using (16).

$$U_{\max}[dB\mu V] = 20\log[1/\mu V \sum_{f=MB-\frac{BW}{2}}^{f=MB+\frac{BW}{2}} U_{meas}(f)\cdot RBW(f)] \quad (16)$$

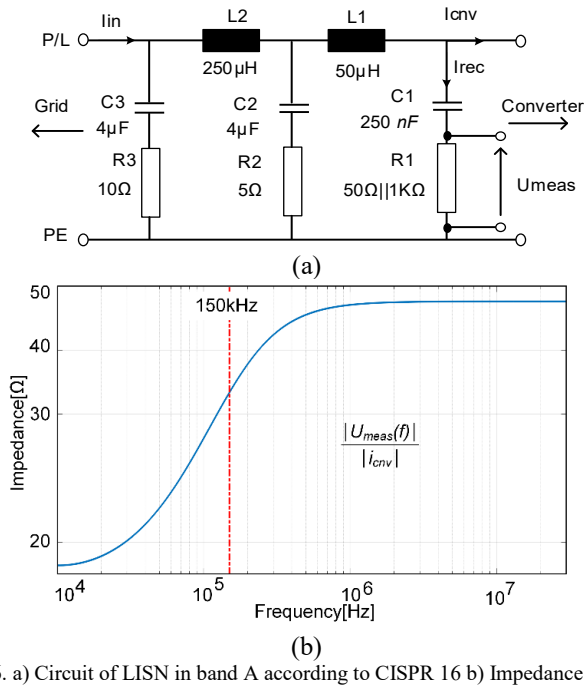


Fig. 6. a) Circuit of LISN in band A according to CISPR 16 b) Impedance frequency behavior of LISN.

## III. Comparitive Results

In order to evaluate the proposed modelling, the PFC rectifier shown in Fig. 2 is considered under Continuous Conduction Mode (CCM) as it is summarized in Table I. Two simulation cases are considered to show the 9–150 kHz EMI performance of the PFC rectifier with different switching frequencies. The type of LISN for measurement of low-frequency EMI is ESH2-Z5 (9 kHz-30 MHz) and also the digital oscilloscope model, which is used in the experimental set up is LeCroy Wave Surfer 3024-200 MHz (4 channels). Moreover, the EMI receiver analyser model is N9010A EXA. A photograph of these instruments is shown in Fig. 7.

The switching model has been run in PLECS software. The sampling frequency of simulation and experimental results is 100 kHz. Fig. 8 shows the obtained experimental, analytical and switching model for EMI peak measurement (Band A) with switching frequency of $f_{sw}$ = 20 kHz. As it can be seen, the analytical model exactly matches the switching simulation model and the error is less than 1 dB in the main harmonics. Moreover, the obtained results not only confirm the effectiveness of the analytical modeling method but also easy to investigate system level EMI and design of EMI filter for the converter. According to Fig. 8, experimental results confirm the analytical and switching model for EMI at low frequencies, where, obviously the modeling error is under 1.2 dB. Table. II presents the results of differential mode EMI and error of experimental, simulation and analytical models. It is clear that the error of the proposed model is not considerable.

The second case study has been simulated and modeled to further investigate the analytical model effectiveness. Fig. 9 shows the experimental input current, voltage and output voltage waveforms of the single-phase PFC rectifier for the case of switching frequency equal to 25 kHz. The EMI peak measurement is shown in Fig. 10. According to Fig. 10, the experimental results confirm the analytical and switching model for low frequency EMI with switching frequency of 25 kHz. Finally, Table. III presents the results of differential mode EMI and error due to experimental, simulation and analytical models for whole range of current harmonics. Moreover, the error has been calculated for models with a comparison with each other. It is also important to highlight that the error of the analytical model at low-frequency EMI is negligible.

TABLE I. Case Study Specification.

| Symbol | Parameter | Value | Unit of Measuring |
|---|---|---|---|
| $U_{IN}$ | Grid phase voltage | 230 | $V_{rms}$ |
| $F_G$ | Grid frequency | 50 | Hz |
| $L$ | DC link inductor | 1.8 | mH |
| $F_{SW}$ | Switching Frequency | 20,25 | kHz |
| $C_{DC}$ | DC link capacitor | 500 | µF |
| $U_{DC}$ | Output voltage | 400 | V |
| $PO$ | Output power | 1 | kW |

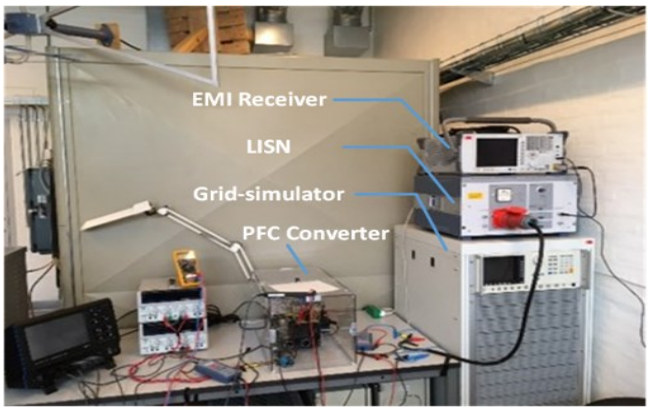


Fig. 7. Photograph of the test setup for Boost PFC converter.

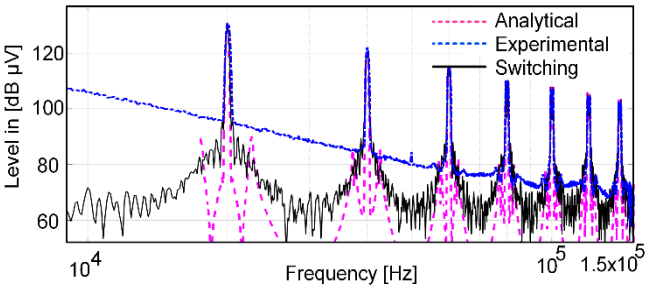


Fig. 8. Obtained eperimental and analytical and switching model for EMI peak measurement (Band A) with switching frequency (fsw = 20 kHz).

TABLE II. Obtained Comparative Differential Mode Noise Values for Quasi-Peak Measermrnt, Simulationa and Proposed Analytical Approach at 20 kHz.

| Boost PFC in CCM operation case(fsw = 20 kHz) | | | | | | |
|---|---|---|---|---|---|---|
| $f_D$ | *Experimental [dB]* | *Analytical [dB]* | *Simulation [dB]* | $E_{A\text{-}E}$ *[dB]* | $E_{S\text{-}E}$ *[dB]* | $E_{S\text{-}A}$ *[dB]* |
| 1 | 130.63 | 129.7 | 129.6 | 0.93 | 1.03 | 0.1 |
| 2 | 121.7 | 120.5 | 120.25 | 1.2 | 0.55 | 0.25 |
| 3 | 114.5 | 113.5 | 114.4 | 1 | 0.1 | 0.9 |
| 4 | 109.68 | 108.75 | 109.1 | 0.93 | 0.58 | 0.35 |
| 5 | 105.82 | 106.4 | 106.6 | 0.58 | 0.78 | 0.2 |
| 6 | 104.3 | 103.7 | 104.2 | 0.6 | 0.1 | 0.5 |
| 7 | 102.3 | 102 | 101.8 | 0.3 | 0.5 | 0.2 |

$F_D$: Difrentioal frequency
$E_{S\text{-}E}$: Error for simulation and experimental
$E_{A\text{-}E}$: Error for analytical and experimental
$E_{S\text{-}A}$: Error for simulation and analytical

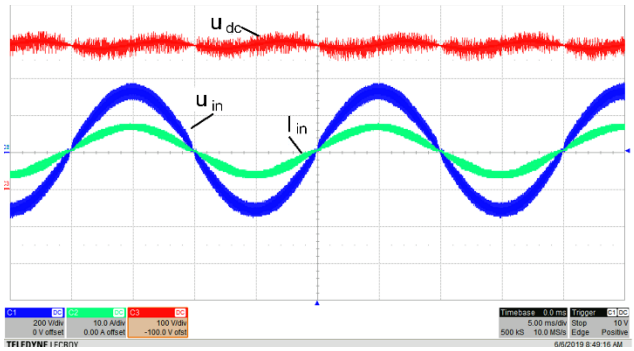


Fig. 9. Measured experimental waveform of a single phase PFC rectifier with following Table1($f_{sw}$= 25 kHz).

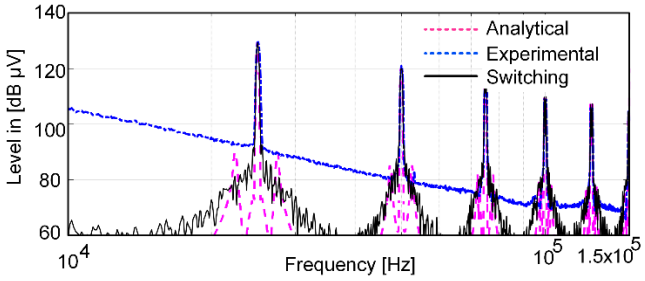


Fig. 10. Obtained eperimental, analytical and switching model for EMI peak measurement (Band A) with switching frequency of *fsw* = 25 kHz.

TABLE III. OBTAINED COMPARATIVE DIFFERENTIAL MODE NOISE VALUES FOR QUASI-PEAK MEASERMRNT, SIMULATIONA AND PROPOSED ANALYTICAL APPROACH FOR 25 KHZ.

| **BOOST PFC IN CCM OPERATION CASE(FSW = 25 KHZ)** | | | | | | |
|---|---|---|---|---|---|---|
| $f_D$ | *Experimental [dB]* | *Analytical [dB]* | *Simulation [dB]* | $E_{A-E}$ *[dB]* | $E_{S-E}$ *[dB]* | $E_{S-A}$ *[dB]* |
| 1 | 129.48 | 129.47 | 129.39 | 0.01 | 0.09 | 0.08 |
| 2 | 121 | 120.2 | 120 | 0.8 | 1 | 0.2 |
| 3 | 113.6 | 112.68 | 113.2 | 0.92 | 0. 4 | 0.52 |
| 4 | 109 | 108.6 | 109.5 | 0.4 | 0. 5 | 0.9 |
| 5 | 104.5 | 105.75 | 105.5 | 1.25 | 1 | 0.25 |
| 6 | 104.5 | 104.3 | 104.8 | 0.2 | 0.3 | 0.5 |

## IV. CONCLUSION

In this paper, an analytical technique for low-frequency EMI modelling in a boost PFC converter has been proposed. The proposed analytical model has been investigated for two different switching frequencies. Moreover, the presented simulation and experimental results have validated the proposed modeling approach. The obtained results show that the error of utilizing the proposed method versus simulation and experimental quasi-peak measurements is less than 1.2 dB at 20 kHz and 1.25 at 25kHz switching frequencies. As a result, the developed analytical approach can provide high accuracy for differential mode EMI noise modelling, which can be employed for EMI filter design and investigation of EMI emissions at large scale systems.

## REFERENCES


[1] J. Ekanayake, K. Liyanage, J. Wu, A. Yokoyama, and N. Jenkins , "Smart Grid Technology and Aplications,". ISBN: 978-0-470-97409-4, no. 306, April 2012.

[2] C. Bennett and D. Highfill, "Networking AMI Smart Meters," *in IEEE Energy*, 2030 Atlanta, Georgia, USA,17-18 November 2008.

[3] F. Benzi, N. Anglani, E. Bassi, and L. Frosini, "Electricity Smart Meters Interfacing The Households," *in IEEE Transactions on Industrial Electronics.*, vol. 58, no. 10, pp. 4487–4494, 2011.

[4] Robert Smolenski, "Conducted Electromagnetic Interference (EMI) in Smart Grids,". ISBN: 9781447129608, 2012.

[5] C.I.S.P.R., *Limits and methods of measurement of radio disturbance characteristics of electrical lighting and similar equipment Interference,* vol. 15, 2015, IEC Int. Special Committee on Radio Interferenc.

[6] P. Davari, E. Hoene, F. Zare, F. Blaabjerg, "Improving 9-150 kHz EMI Performance of Single-Phase PFC Rectifier," *10th International Conference on Integrated Power Electronics Systems*, pp. 512–517, 2018.

[7] Gerhard F. Bartak , A. Abart, "EMI Of Emission In The Frequency Range 2 kHz - 150 kHz," *in 22nd International Conference on Electricity Distribution*, Stockholm, 10-13 June 2013.

[8] M. Kasper, D. Bortis, and J. W. Kolar, "Classification and comparative evaluation of PV panel-integrated DC-DC converter concepts," *in IEEE Transactions on Power Electronics*., vol. 29, no. 5, pp. 2511–2526, 2014.

[9] J. Deng, S. Li, S. Hu, C. C. Mi, and R. Ma, "Design Methodology of LLC Resonant Converters for Electric Vehicle Battery Chargers," *IEEE Transactions on Vehicular Technology*., vol. 63, no. 4, pp. 1581–1592, 2014.

[10] B. K. Lee, J. P. Kim, S. G. Kim, and J. Y. Lee, Member, IEEE, "A PWM SRT DC/DC Converter for 6.6-kW EV Onboard Charger," *IEEE Transactions on industrial electronics*, vol. 63, no. 2, February 2016.

[11] S. Schöttke, J. Meyer, P. Schegner, and S. Bachmann, "Emission in the frequency range of 2 kHz to 150 kHz caused by electrical vehicle charging," *2014 International Symposium on Electromagnetic Compatibility (EMC Europe 2014)*, Gothenburg, Sweden, September 1-4, 2014.

[12] E. O. A. Larsson, M. H. J. Bollen, M. G. Wahlberg, C. M. Lundmark, and S. K. Rönnberg, "Measurements of High-Frequency (2–150 kHz) Distortion in Low-Voltage Networks," *IEEE Transactions on Power Delivery*, vol. 25, no. 3, pp. 1749–1757, 2010.

[13] D. Boillat, F. Krismer, and J. Kolar, "EMI Filter Volume Minimization of a Three-Phase/Level T-Type PWM Converter System," *IEEE Transaction on Power Electronic.*, vol.32, pp. 2473 - 2480, April 2017.

[14] H. Bishnoi, A. C. Baisden, P. Mattavelli, and D. Boroyevich, "Analysis of EMI terminal modeling of switched power converters," *IEEE Transactions on Power Electronics.*, vol. 27, no. 9, pp. 3924–3933, September 2012.

[15] J. Espina, J. Balcells, A. Arias, and C. Ortega, "EMI modeling method of AC-AC power converters," *IEICE Electronics Express*., vol. 8, no. 1, pp. 13–19, 2011.

[16] J. Sun, "Input Impedance Analysis of Single-Phase PFC Converters," *IEEE Transactions on Power Electronics*, vol. 20 , pp. 308 - 314, March 2005.

[17] C.I.S.P.R., *Specification for Radio Interference Measuring Apparatus and Measurement Methos Publication 16*, 2015, p. IEC Int. Special Committee on Radio Interferenc.

[18] T. Nussbaumer, M.L. Heldwein, J.W. Kolar, "Differential Mode Input Filter Design for a Three-Phase Buck-Type PWM Rectifier Based on Modeling of the EMC Test Receiver," *IEEE Transactions on Industrial Electronics*, vol. 53, pp. 1649-1661 , Issue.5 , October. 2006.